Light penetration structures the deep acoustic scattering layers in the global ocean

Article *in* Science Advances · May 2017

DOI: 10.1126/sciadv.1602468

6 authors, including:

Dag Lorents Aksnes
University of Bergen
120 PUBLICATIONS **4,809** CITATIONS
SEE PROFILE

Anders Røstad
King Abdullah University of Science and Technology
43 PUBLICATIONS **732** CITATIONS
SEE PROFILE

Carlos M. Duarte
King Abdullah University of Science and Technology
968 PUBLICATIONS **54,262** CITATIONS
SEE PROFILE

Xabier Irigoien
AZTI
279 PUBLICATIONS **7,521** CITATIONS
SEE PROFILE

MARINE ECOLOGY

Light penetration structures the deep acoustic scattering layers in the global ocean

Dag L. Aksnes,[1]* Anders Røstad,[2] Stein Kaartvedt,[3] Udane Martinez,[4] Carlos M. Duarte,[2,5] Xabier Irigoien[2†]

The deep scattering layer (DSL) is a ubiquitous acoustic signature found across all oceans and arguably the dominant feature structuring the pelagic open ocean ecosystem. It is formed by mesopelagic fishes and pelagic invertebrates. The DSL animals are an important food source for marine megafauna and contribute to the biological carbon pump through the active flux of organic carbon transported in their daily vertical migrations. They occupy depths from 200 to 1000 m at daytime and migrate to a varying degree into surface waters at nighttime. Their daytime depth, which determines the migration amplitude, varies across the global ocean in concert with water mass properties, in particular the oxygen regime, but the causal underpinning of these correlations has been unclear. We present evidence that the broad variability in the oceanic DSL daytime depth observed during the Malaspina 2010 Circumnavigation Expedition is governed by variation in light penetration. We find that the DSL depth distribution conforms to a common optical depth layer across the global ocean and that a correlation between dissolved oxygen and light penetration provides a parsimonious explanation for the association of shallow DSL distributions with hypoxic waters. In enhancing understanding of this phenomenon, our results should improve the ability to predict and model the dynamics of one of the largest animal biomass components on earth, with key roles in the oceanic biological carbon pump and food web.

INTRODUCTION

The deep scattering layer (DSL) was first identified during World War II as an acoustically dense layer prevalent across the ocean (*1*) and is a prominent signature of marine animal biomass (*2*–*4*). A key feature of the organisms comprising the DSL is their daily migration between the mesopelagic and the oceanic surface layer. A recent study (*3*) reports that, on average, ~50% of the mesopelagic backscatter made daily excursions from mesopelagic depths to shallow waters, although with marked differences (20 to 90%) in migrating proportions between different oceanic regions. Globally, this daily migration involves a living biomass likely larger than 5000 million tons (*3*, *4*), the largest animal migration on Earth, with important consequences for the vertical carbon flux (*2*–*4*) and oceanic food web interactions (*5*). The migration amplitude, which is reflected by the DSL daytime depth, is an integral part and key property of these processes. The DSL daytime depth varies broadly across the global ocean, and recent studies (*3*, *6*) have found that the oxygen regime accounted for most of this variation. Hypoxic water columns tend to have much shallower DSL daytime depth (*6*, *7*) than oxygen-replete water columns, and in some areas, avoidance of hypoxia (*8*, *9*) appears to be the cause for the variation in DSL daytime depth and, consequently, migration amplitude. However, observations from the Malaspina Circumnavigation Expedition, which assessed DSL across the global tropical ocean (*3*, *4*), showed that most of the acoustic backscatter (a proxy for biomass) was located deep into the hypoxic and also into the anoxic layer in areas with anoxia, suggesting that avoidance of hypoxia cannot be a general driver for shallow DSL distributions. These acoustic observations were made at 38 kHz and do not encompass all mesopelagic animals but are considered to be geared toward the larger micronektonic components that are acoustically detectable, particularly mesopelagic fish with a gas-filled swim bladder (*3*, *4*).

Since the DSL was first detected, variations in incoming sunlight have been proposed as the proximate driver for the daily vertical migration (*10*, *11*). Current theoretical frameworks explain the daily migration as a behavior to continuously track light intensities that best meet the compromise between the ability to feed and to minimize the risk of being eaten by visual predators (*12*, *13*). The resulting light interval occupied by mesopelagic fishes has been referred to as the light comfort zone (LCZ) (*14*, *15*). In theory, an LCZ, which is conserved across oceans with variable light penetration, implies that the DSL daytime depth should distribute proportionally to the reciprocal light attenuation coefficient for downwelling irradiance (*14*, *15*), that is, in a specific optical depth layer. However, whether a common LCZ can account for the global variation in DSL daytime depth has not been investigated. Previous studies, which have addressed the potential role of light penetration on DSL distribution, have applied surface water–associated proxies for light penetration, such as Secchi depth (*16*), chlorophyll a concentration (*17*), and satellite-observed ocean color (*6*), all of which carry considerable uncertainty in representing light penetration at mesopelagic depths (*14*, *15*, *18*). Here, we combine for the first time DSL observations on a global scale (Fig. 1A) with direct underwater irradiance measurements down to depths of 150 to 280 m (depending on water clarity). We test the hypothesis that the daytime depth range occupied by DSL organisms is set by light penetration and conforms to a specific optical depth layer (referred to as the LCZ hypothesis).

RESULTS

The daytime DSL occupied depth layers with large variation in oxygen concentration but with comparable light intensities (Fig. 1). As a consequence, the daytime acoustic backscatter was distributed broadly across both the mesopelagic depth range of 200 to 1000 m (Fig. 2A and fig. S2) and the observed range of dissolved oxygen (0 to 5.6 ml liter^{-1}; Fig. 2B), pointing to no clear constraint of depth or dissolved oxygen on the position of the DSL. In contrast, the acoustic backscatter is restricted to a

[1]Department of Biology and Hjort Centre for Marine Ecosystem Dynamics, University of Bergen, Bergen, Norway. [2]Red Sea Research Center, King Abdullah University of Science and Technology, Thuwal 23955-6900, Saudi Arabia. [3]Department of Biosciences, University of Oslo, Oslo, Norway. [4]AZTI, Arrantza eta Elikaigintzarako Institutu Teknologikoa, Herrera Kaia Portualdea, 20110 Pasaia, Spain. [5]Arctic Research Centre, Department of Bioscience, Aarhus University, C.F. Møllers Allé 8, DK-8000 Århus C, Denmark
*Corresponding author. Email: dag.aksnes@uib.no
†Present addresses: AZTI–Marine Research, Herrera Kaia, Portualdea z/g, 20110 Pasaia (Gipuzkoa), Spain, and Ikerbasque, Basque Foundation for Science, Bilbao, Spain.

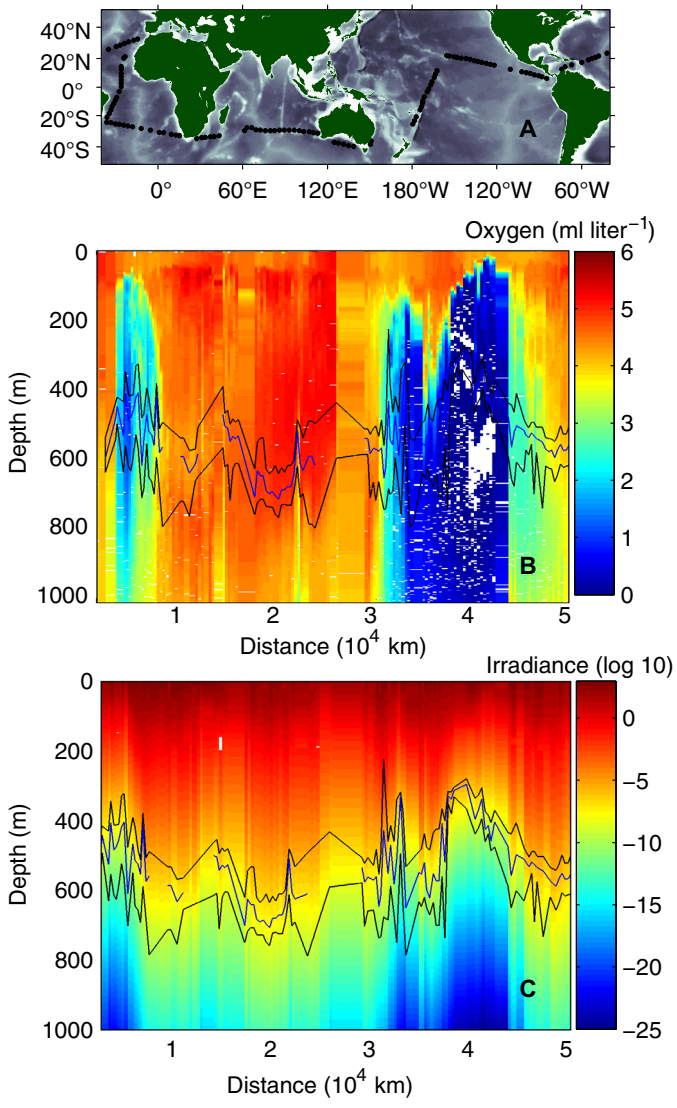

Fig. 1. The Malaspina 2010 Circumnavigation Expedition. The stations along the cruise track (**A**). Dissolved oxygen concentration (**B**) and downwelling irradiance (**C**) in the visible spectrum (400 to 700 nm) in µmol quanta m^{-2} s^{-1} (logarithmic scale). Daytime DSL weighted median depths (blue line) with 25 and 75% quartiles (black lines) are indicated in (B) and (C). Downwelling irradiance was measured down to depths of 180 to 280 m and calculated according to a proxy model (see Materials and Methods) of light attenuation beyond. Distance is the distance traveled along the cruise track from the first station.

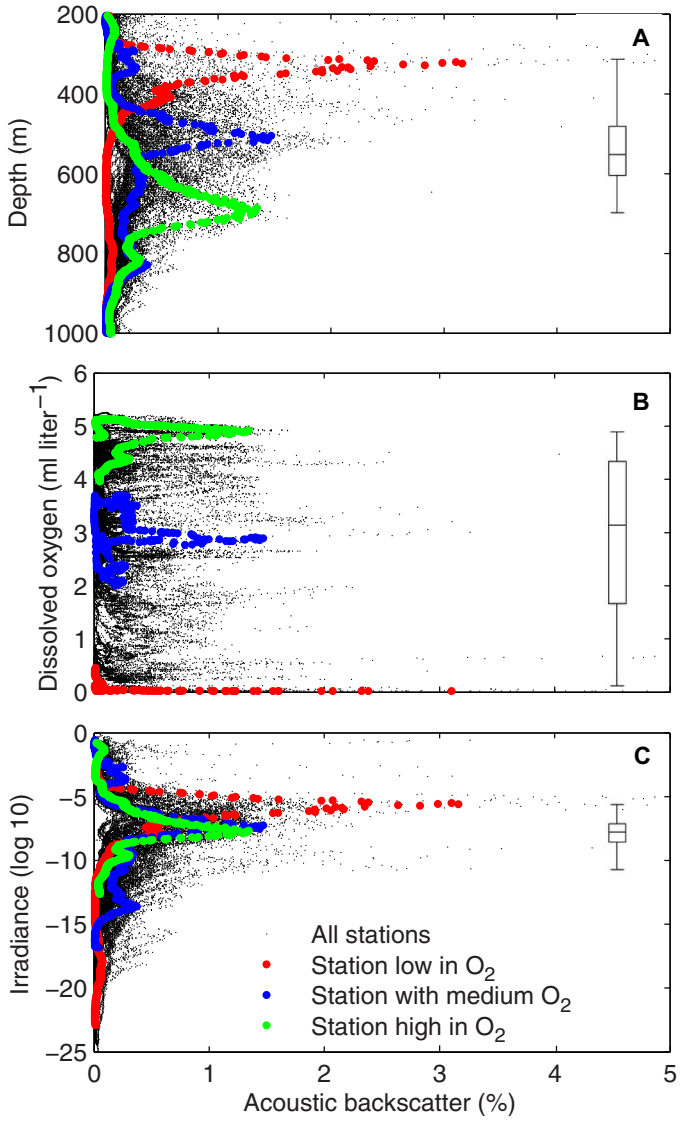

Fig. 2. Daytime distribution of acoustic backscatter in the mesopelagic (200 to 1000 m). Percentage acoustic backscatter as a function of depth (**A**), ambient dissolved oxygen concentration (**B**), and ambient irradiance (**C**) of the backscatter. Black dots are data from all stations, and each dot represents the acoustic backscatter of a 2-m depth interval at a particular station as a percentage of total backscatter between 200 and 1000 m at that station. The acoustic backscatter marked in colors are from three stations with different oxygen regimes: low oxygen (Pacific Ocean, 15.9°N, 124.5°W), medium oxygen (Atlantic Ocean, 11.7°S, 31.4°W), and high oxygen (Indian Ocean, 29.6°S, 89.4°E). The boxplots show median, quartiles, and the range of the DSL WMDs for all stations.

narrow range of mesopelagic daytime irradiance compared to the total span in mesopelagic daytime irradiance (Fig. 2C). Along the cruise track, the mesopelagic (200 to 1000 m) irradiance spanned 25 orders of magnitude (Fig. 2C), from 0.8 µmol quanta m^{-2} s^{-1} at 200-m depth at the clearest station to an extrapolated minimum of 10^{-25} µmol quanta m^{-2} s^{-1} at 1000-m depth at the darkest station. This extrapolated light intensity is purely theoretical and much lower than, for instance, ambient bioluminescent light. Nevertheless, compared with 10^{-13} µmol quanta m^{-2} s^{-1} at 1000 m at the clearest station, this shows that the total span of 0.033 to 0.064 m^{-1} in the average light attenuation coefficient (K_I, between surface and 1000-m depth), which might appear modest, has major effects on the mesopelagic light regime.

The average light intensity at the median depth of the DSL distribution for all stations was around 10^{-7} µmol quanta m^{-2} s^{-1} with a span from 10^{-6} to 10^{-9} µmol quanta m^{-2} s^{-1} at the 25 and 75% quartile DSL depths, respectively. In line with the predictions of the LCZ hypothesis (*14*, *15*), the weighted mean depth (WMD) of the DSL distribution of the stations increased linearly with the reciprocal of the light attenuation coefficient. This linear relationship was found when the light attenuation coefficient was estimated for the entire water column down to 1000 m (K_I; Fig. 3A) by using the empirical light attenuation model depth (table S1), but also when it was estimated from

actual light measurements only, that is, for the water column shallower than the 0.01% light depth ($K_{0.01\%}$; Fig. 3B). This strong relationship further confirms the role of light penetration as a driver of the depth distribution of the mesopelagic DSL. We note that the modeled attenuation coefficient, representing the entire water column (K_I), accounted for 20% more of the variation in WMD (Fig. 3A) than the one ($K_{0.01\%}$) representing the measurements in the upper water column (Fig. 3B).

DISCUSSION

Association between light penetration and oxygen regime

The lack of association between the mesopelagic backscatter and ambient oxygen concentration (Fig. 2B and fig. S2B) might appear contradictory with previous reports that show the relationship between DSL distribution and oxygen (*3*, *6*–*8*). However, our results are consistent with these studies because oxygen-rich Indian Ocean and hypoxic eastern Pacific Ocean waters are characterized by a deep and a shallow DSL, respectively (Fig. 2B), with the DSL of the South Atlantic Ocean characterized by an intermediate oxygen regime being located at intermediate depths. Although this confirms a broad association between the DSL daytime depth and the oxygen regime in the global ocean, our observations provide no evidence for a common preference for dissolved oxygen across the ocean. In contrast, restriction of the DSL to a specific irradiance regime (Fig. 2C) offers a more parsimonious and universal explanation for variation in DSL depth in different waters. Hence, our results suggest that the overall association between DSL and oxygen is due to a negative relationship between light attenuation and dissolved oxygen (table S1 and figs. S3 and S4), involving reduced light penetration in the mesopelagic zone in hypoxic water columns compared to that in oxygen-replete waters. We note that although fluorescence is the most important proxy for the observed light attenuation shallower than 100-m depth, dissolved oxygen becomes increasingly more important than fluorescence for water masses deeper than 100 m (table S2). A pronounced negative correlation between light attenuation and dissolved oxygen has been reported in the past for the mesopelagic layer of deep fjords (*19*, *20*). Furthermore, our results are consistent with previous studies (*21*, *22*) showing that the concentration of colored (or chromophoric) dissolved organic matter (CDOM), which is an important light absorber (*21*), is closely associated with high oxygen deficiency (given as apparent oxygen utilization) across the ocean. Thus, the mechanism underlying the association between the light attenuation coefficient and dissolved oxygen might involve the release of CDOM as a result of microbial heterotrophic degradation of particulate organic matter, resulting in elevated light attenuation in oxygen-depleted mesopelagic waters (*19*, *22*).

Implications of the expected expansion of the oceanic oxygen minimum zones

The oxygen minimum zones of the worlds' oceans are expected to expand both horizontally and vertically with ocean warming (*23*) and have been suggested, consequently, to force mesopelagic organisms upward (*8*, *9*). Although our results point at light penetration rather than oxygen as a driver for DSL positioning also in oxygen-depleted water, this expectation remains the same in our study because of the correlation between dissolved oxygen and light attenuation. However, our data suggest that the shallow DSL distributions are not exposed to higher light intensities than the deep DSL distributions and, therefore, should not render the mesopelagic fauna more vulnerable to visual predators (*8*, *9*). On the contrary, the shallow DSL in oxygen-depleted water remains embedded within hypoxic layers, which might reduce the vulnerability to fish predators.

Ambient light of the DSL in relation to visual thresholds

The daytime twilight environment at the median DSL depth reported here (10^{-7} µmol quanta m^{-2} s^{-1}) is quite low—comparable to that of a moonless, partially cloudy starry night (10^{-10} dimmer than daylight) and about 10,000 times dimmer than the surface light received on a clear sky, full moon night (*24*). Although accurate assessment of the visual environment requires wavelength resolution (*25*), which is likely

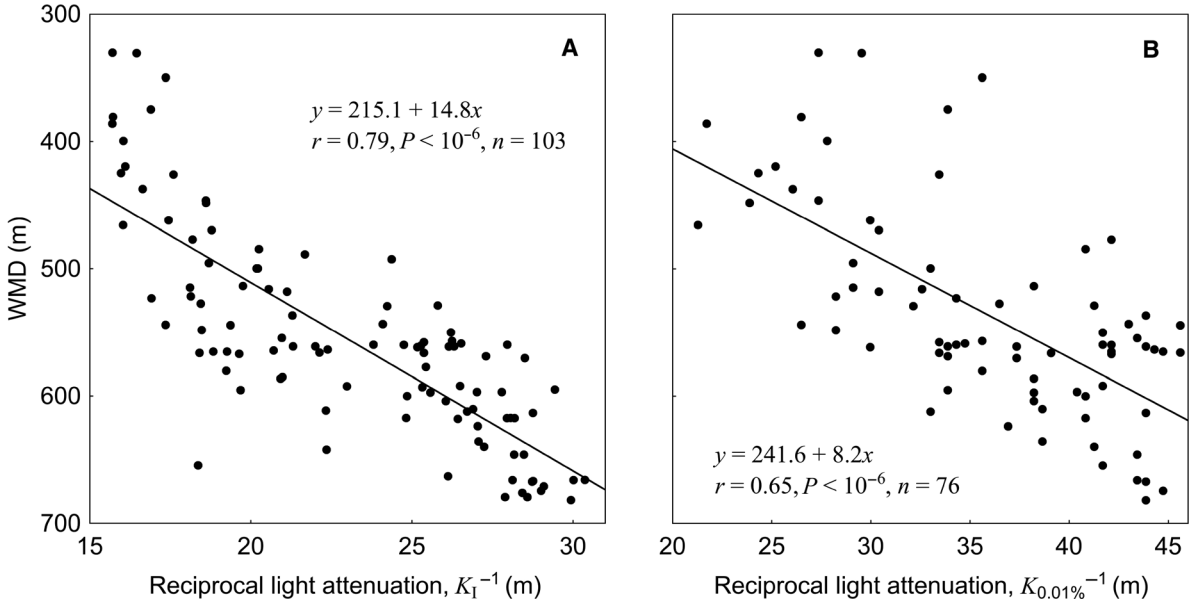

Fig. 3. DSL daytime depth in relation to light penetration. The WMD of the DSL plotted against the reciprocal light attenuation coefficient that is (**A**) modeled (K_I) for the entire water column down to 1000-m depth and (**B**) estimated ($K_{0.01\%}$) from irradiance measurements conducted in the upper water masses down to 0.01% light depth.

to be dominated by blue at the DSL, we note that the irradiance at the median DSL depth found here was similar to reported absolute visual thresholds for predator teleost fish (about 10^{-6} µmol quanta m^{-2} s^{-1}) (*26*) but 100-fold higher than the visual thresholds for mesopelagic fish [about 10^{-9} µmol quanta m^{-2} s^{-1} for the lanternfish (*25*)]. The DSL does not occur as a narrow layer but as a broad (100 to 200 m thick) band (fig. S2) encompassing a range of light levels that may be structured by the diversity of light thresholds of the species conforming the DSL.

Possible effect of the light regime on carbon export

The finding that the positioning of the DSL in the water column is structured by water column light penetration provides a major insight into the biogeochemical functioning of the ocean. Highly transparent oceanic waters, such as those that characterize the subtropical oligotrophic gyres comprising 70% of the open ocean, would lead to daytime DSL depths approaching the base of the mesopelagic layer at 1000-m depth (*3*). Feeding of the DSL animals near the surface of the oligotrophic ocean at night would then lead to a transport of the ingested organic carbon that is subsequently respired and defecated at depth, down to the base of the mesopelagic layer in a matter of a few hours, thereby accelerating the downward flux of carbon. This transport would otherwise require weeks to months to reach such depths, implying much organic carbon remineralization while sinking (*27*, *28*). The finding reported here, that the DSL depth is controlled by water column light penetration, identifies a carbon shunt mechanism that is affected by the light regime. Although it has been reported (*3*) that the migrating fraction of mesopelagic fauna is smaller for deep than for shallow DSL, this clear-water carbon shunt bypasses the remineralization layer in transit through the upper and mesopelagic ocean to directly inject fresh carbon derived from the ocean surface at the base of the mesopelagic layer. Given the huge mesopelagic biomass (*3*, *4*), this is of consequence, because it should result in high efficiency of carbon sequestration relative to primary production in the clear oligotrophic ocean, as hypothesized recently (*4*), while also effectively linking primary production in the upper water to the food web in the deep ocean.

MATERIAL AND METHODS

The Malaspina 2010 Circumnavigation Expedition sailed the subtropical and tropical open ocean between December 2010 and July 2011, sampling the Atlantic, Indian, and Pacific Oceans (Fig. 1A) (*29*).

Echosounder

Acoustic data were recorded continuously during the cruise using a calibrated 38-kHz Simrad EK60 (7° beam width) echosounder. The ping rate was one transmitted pulse per 2 s. The acoustic data were occasionally affected by noise and were filtered and scrutinized, as outlined by Irigoien *et al.* (*4*). Data were integrated in 2-m depth bins at a threshold of −90 dB. We averaged each depth bin at daytime (1 hour after sunrise to 1 hour before sunset) for each day and linked the data to the corresponding conductivity-temperature-depth (CTD) cast, which included underwater irradiance measurements at daytime, with a maximum time difference of 24 hours. We have used nautical area scattering coefficients [NASC; s_A (m^2 nautical $mile^{-2}$)] as the measurement for the acoustic backscatter. To standardize the data for each CTD station, we divided the NASC of each depth bin by the total NASC at that station and called fraction NASC (%). The weighted mean and median depths and percentiles were calculated from these data. These calculations and Figs. 1 to 3 were carried out in Matlab.

Light measurements

An upward facing LI-COR Biospherical PAR (photosynthetically active radiation) (400 to 700 nm) sensor was attached to a Rosette sampling system containing a CTD probe and other sensors. Downwelling irradiance in the visible band was registered around noon for each second meter. Another sensor located at the ship provided simultaneous registrations of air irradiance. The underwater irradiance was measured accurately to a minimal level of 0.03 µmol quanta m^{-2} s^{-1}. This intensity corresponded to the daytime irradiance at depths of 150 to 280 m, depending on the actual water clarity at the location.

Salinity, dissolved oxygen, fluorescence, and turbidity

Salinity (practical salinity unit), dissolved oxygen (electronic measurements in units of ml $liter^{-1}$), fluorescence (relative units), and turbidity (relative units obtained by a Seapoint Turbidity Meter measuring light scattered by particles) were recorded for each second meter simultaneously with the light measurements.

Model of the observed light attenuation coefficient

To calculate the ambient irradiance of acoustic scatter at depths deeper than the available underwater light measurements, we derived an empirical model of the observed light attenuation coefficient. This derivation involved two steps: (i) calculation of the depth-specific light attenuation coefficient (K_s), for each second meter, from the underwater light measurements conducted deeper than 60 m and (ii) use of a multiple regression model that related the observed K_s to the simultaneous measurements of salinity, oxygen, fluorescence, and turbidity. The reason for using observed attenuation coefficients below 60 m is twofold. First, at this depth, a large fraction of the downwelling irradiance is diffuse, which makes the light attenuation coefficient less affected by variation in the angular distribution of light. Second, the wavelength distribution of the downwelling irradiance at this depth has narrowed into a band that is more relevant for the mesopelagic than the wavelength composition of upper water irradiance. Hence, although a PAR (400 to 700 nm) sensor was applied, the K_s values reflect a narrower band closer to that of the mesopelagic layer.

At each station, the underwater light measurements $E(z)$ at depth z were divided by the simultaneous air measurement, E_{surf}, that is, $f(z) = E(z)/E_{surf}$, where $f(z)$ is the fraction of the light that penetrated down to depth z. The depth-specific attenuation coefficients, K_s, were estimated as the slope in a linear regression analysis of $\ln(f)$ versus z. Seven $\ln(f)$ values, representing a 12-m depth layer, were included in each of these regressions [for example, K_s for 70-m depth was estimated from the $\ln(f)$ values at 64-, 66-, 68-, 70-, 72-, 74-, and 76-m depth]. The estimated K_s values were sensitive to anomalous light measurements, which in some cases could result in, for example, negative K_s values. To minimize the number of erroneous K_s values, we applied only estimates with a squared correlation coefficient higher than 0.99.

According to previous studies, which have shown correlations between nonchlorophyll light absorption or light attenuation on the one hand and salinity and dissolved oxygen on the other (*19*–*22*), measurements of dissolved oxygen and salinity were included with fluorescence and turbidity as independent variables in a multiple regression analysis, with K_s as the dependent variable. Measurements of salinity, oxygen, fluorescence, and turbidity were simultaneous with the light measurements (and thereby the K_s values) because they were obtained from the same CTD casts. Light attenuation is known to relate nonlinearly with chlorophyll, and before the multiple regression analysis (table S1), the fluorescence value, F, was transformed; $F^{0.428}$, according to a previously reported (*30*) relationship.

Calculation of the ambient light of the acoustic scatter

In cases where mesopelagic acoustic scatter was shallower than the deepest light measurement, we set the ambient light of the acoustic scatter equal to the measured light at same depth. At depths below the deepest light measurement, we approximated the ambient light by using the empirical light attenuation model that is explained above. For example, if the depth of the deepest irradiance measurement at a station was 240 m, the irradiance at 242-m depth was calculated as $E(242) = E(240)\exp(-K_{proxy}(240)(242 - 240))$, where $K_{proxy}(240)$ was obtained by insertion of the measured salinity, dissolved oxygen, chlorophyll, and turbidity at 240-m depth in the proxy model (table S1). This procedure was repeated for each second meter throughout the mesopelagic layer down to a depth of 1000 m. At some occasions, the turbidity measurements were unreliable (extremely high values) and only records with turbidity <0.12 were used in the calculation of K_{proxy}.

SUPPLEMENTARY MATERIALS

Supplementary material for this article is available at http://advances.sciencemag.org/cgi/content/full/3/5/e1602468/DC1

table S1. Model of the observed light attenuation coefficient.

table S2. Linear regression analyses of the depth-specific light attenuation coefficient versus fluorescence or dissolved oxygen.

fig. S1. The observed depth-specific light attenuation coefficient versus that approximated from the multiple regression model.

fig. S2. DSL distribution along the cruise track.

fig. S3. Association between the depth-specific light attenuation coefficient and the dissolved oxygen concentration.

fig. S4. Observations of fluorescence, dissolved oxygen concentration, and depth-specific light attenuation coefficient.

REFERENCES AND NOTES

1. R. Carson, *The Sea Around Us* (Oxford Univ. Press, 1951).
2. P. C. Davison, D. M. Checkley Jr., J. A. Koslow, J. Barlow, Carbon export mediated by mesopelagic fishes in the northeast Pacific Ocean. *Prog. Oceanogr.* **116**, 14–30 (2013).
3. T. A. Klevjer, X. Irigoien, A. Røstad, E. Fraile-Nuez, V. M. Benítez-Barrios, S. Kaartvedt, Large scale patterns in vertical distribution and behaviour of mesopelagic scattering layers. *Sci. Rep.* **6**, 19873 (2016).
4. X. Irigoien, T. A. Klevjer, A. Røstad, U. Martinez, G. Boyra, J. L. Acuña, A. Bode, F. Echevarria, J. I. Gonzalez-Gordillo, S. Hernandez-Leon, S. Agusti, D. L. Aksnes, C. M. Duarte, S. Kaartvedt, Large mesopelagic fishes biomass and trophic efficiency in the open ocean. *Nat. Commun.* **5**, 3271 (2014).
5. A. N. Kozlow, A review of the trophic role of mesopelagic fish of the family Myctophidae in the Southern Ocean ecosystem. *CCAMLR Sci.* **2**, 71–77 (1995).
6. D. Bianchi, E. D. Galbraith, D. A. Carozza, K. A. S. Mislan, C. A. Stock, Intensification of open-ocean oxygen depletion by vertically migrating animals. *Nat. Geosci.* **6**, 545–548 (2013).
7. A. N. Netburn, A. J. Koslow, Dissolved oxygen as a constraint on daytime deep scattering layer depth in the southern California current ecosystem. *Deep-Sea Res. I Oceanogr. Res. Pap.* **104**, 149–158 (2015).
8. J. A. Koslow, R. Goericke, A. Lara-Lopez, W. Watson, Impact of declining intermediate-water oxygen on deepwater fishes in the California Current. *Mar. Ecol.: Prog. Ser.* **436**, 207–218 (2011).
9. W. F. Gilly, J. M. Beman, S. Y. Litvin, B. H. Robison, Oceanographic and biological effects of shoaling of the oxygen minimum zone. *Ann. Rev. Mar. Sci.* **5**, 393–420 (2013).
10. E. M. Kampa, B. P. Boden, Submarine illumination and the twilight movements of a sonic scattering layer. *Nature* **174**, 869–871 (1954).
11. H. S. J. Roe, Vertical distributions of euphausiids and fish in relation to light intensity in the Northeastern Atlantic. *Mar. Biol.* **77**, 287–298 (1983).
12. C. W. Clark, D. A. Levy, Diel vertical migrations by juvenile sockeye salmon and the antipredation window. *Am. Nat.* **131**, 271–290 (1988).
13. R. Rosland, J. Giske, A dynamic optimization model of the diel vertical distribution of a pelagic planktivorous fish. *Prog. Oceanogr.* **34**, 1–43 (1994).
14. A. Røstad, S. Kaartvedt, D. L. Aksnes, Light comfort zones of mesopelagic acoustic scattering layers in two contrasting optical environments. *Deep-Sea Res. I Oceanogr. Res. Pap.* **113**, 1–6 (2016).
15. A. Røstad, S. Kaartvedt, D. L. Aksnes, Erratum to "Light comfort zones of mesopelagic acoustic scattering layers in two contrasting optical environments" [Deep-Sea Res. I 113 (2016) 1–6]. *Deep-Sea Res. I Oceanogr. Res. Pap.* **114**, 162–164 (2016).
16. R. R. Dickson, On the relationship between ocean transparency and the depth of sonic scattering layers in the North Atlantic. *ICES J. Mar. Sci.* **34**, 416–422 (1972).
17. S. Kaartvedt, W. Melle, T. Knutsen, H. R. Skjoldal, Vertical distribution of fish and krill beneath water of varying optical properties. *Mar. Ecol. Prog. Ser.* **136**, 51–58 (1996).
18. E. Norheim, T. A. Klevjer, D. L. Aksnes, Evidence for light-controlled migration amplitude of a sound scattering layer in the Norwegian Sea. *Mar. Ecol. Prog. Ser.* **551**, 45–52 (2016).
19. D. L. Aksnes, N. Dupont, A. Staby, Ø. Fiksen, S. Kaartvedt, J. Aure, Coastal water darkening and implications for mesopelagic regime shifts in Norwegian fjords. *Mar. Ecol. Prog. Ser.* **387**, 39–49 (2009).
20. D. L. Aksnes, Sverdrup critical depth and the role of water clarity in Norwegian Coastal Water. *ICES J. Mar. Sci.* **72**, 2041–2050 (2015).
21. N. B. Nelson, D. A. Siegel, The global distribution and dynamics of chromophoric dissolved organic matter. *Ann. Rev. Mar. Sci.* **5**, 447–476 (2013).
22. T. S. Catalá, I. Reche, M. Álvarez, S. Khatiwala, E. F. Guallart, V. M. Benítez-Barrios, A. Fuentes-Lema, C. Romera-Castillo, M. Nieto-Cid, C. Pelejero, E. Fraile-Nuez, E. Ortega-Retuerta, C. Marrasé, X. A. Álvarez-Salgado, Water mass age and aging driving chromophoric dissolved organic matter in the dark global ocean. *Global Biogeochem. Cycles* **29**, 917–934 (2015).
23. G. Shaffer, S. M. Olsen, J. O. P. Pedersen, Long-term ocean oxygen depletion in response to carbon dioxide emissions from fossil fuels. *Nat. Geosci.* **2**, 105–109 (2009).
24. E. J. Warrant, N. A. Locket, Vision in the deep sea. *Biol. Rev.* **79**, 671–712 (2004).
25. J. R. Turner, E. M. White, M. A. Collins, J. C. Partridge, R. H. Douglas, Vision in lanternfish (Myctophidae): Adaptations for viewing bioluminescence in the deep-sea. *Deep-Sea Res. I Oceanogr. Res. Pap.* **56**, 1003–1017 (2009).
26. A. W. Stoner, Effects of environmental variables on fish feeding ecology: Implications for the performance of baited fishing gear and stock assessment. *J. Fish Biol.* **65**, 1445–1471 (2004).
27. A. L. Shanks, J. D. Trent, Marine snow: Sinking rates and potential role in vertical flux. *Deep-Sea Res. I Oceanogr. Res. Pap.* **27**, 137–143 (1980).
28. J. T. Turner, Zooplankton fecal pellets, marine snow, phytodetritus and the ocean's biological pump. *Prog. Oceanogr.* **130**, 205–248 (2015).
29. C. M. Duarte, Seafaring in the 21st century: The Malaspina 2010 Circumnavigation Expedition. *Limnol. Oceanogr.* **24**, 11–14 (2015).
30. A. Morel, Optical modeling of the upper ocean in relation to its biogenous matter content (case I waters). *J. Geophys. Res.* **93**, 10749–10768 (1988).

Acknowledgments: We thank the reviewers for their constructive suggestions. **Funding:** This is a contribution to the Malaspina 2010 Circumnavigation Expedition project, funded by the CONSOLIDER-Ingenio 2010 program from the Spanish Ministry of Economy and Competitiveness (ref. CSD2008-00077). Additional funding was provided by King Abdullah University of Science and Technology through the baseline program. **Author contributions:** D.L.A., A.R., S.K., and X.I. conceived this study. U.M., X.I., and C.M.D. organized the collection of the data. A.R. and D.L.A. analyzed the data. D.L.A., A.R., S.K., C.M.D., and X.I. wrote and edited the paper. All authors discussed the results and commented on the manuscript. **Competing interests:** The authors declare that they have no competing interests. **Data and materials availability:** Data used in the present paper is deposited at the Malaspina database (http://metamalaspina.imedea.uib-csic.es/geonetwork/srv/en/main.home).

Submitted 8 October 2016
Accepted 13 April 2017
Published 31 May 2017
10.1126/sciadv.1602468

Citation: D. L. Aksnes, A. Røstad, S. Kaartvedt, U. Martinez, C. M. Duarte, X. Irigoien, Light penetration structures the deep acoustic scattering layers in the global ocean. *Sci. Adv.* **3**, e1602468 (2017).

Light penetration structures the deep acoustic scattering layers in the global ocean
Dag L. Aksnes, Anders Røstad, Stein Kaartvedt, Udane Martinez, Carlos M. Duarte and Xabier Irigoien (May 31, 2017)
Sci Adv 2017, 3:.
doi: 10.1126/sciadv.1602468